

Reconstructing the metric of the local Universe from number counts observations

Sergio Andres Vallejo², Antonio Enea Romano^{1,2}

¹*Theoretical Physics Department, CERN,*

CH-1211 Geneva 23, Switzerland

²*Instituto de Fisica,*

Universidad de Antioquia,

A.A.1226, Medellin, Colombia

Abstract

Number counts observations available with new surveys such as the Euclid mission will be an important source of information about the metric of the Universe. We compute the low red-shift expansion for the energy density and the density contrast using an exact spherically symmetric solution in presence of a cosmological constant. At low red-shift the expansion is more precise than linear perturbation theory prediction. We then use the local expansion to reconstruct the monopole component of the metric from the monopole of the density contrast. We test the inversion method using numerical calculations and find a good agreement within the regime of validity of the red-shift expansion. The method could be applied to observational data to reconstruct the metric of the local Universe with a level of precision higher than the one achievable using perturbation theory.

I. INTRODUCTION

The standard cosmological models is based on the assumption that the Universe is homogeneous and isotropic on sufficiently large scales, and is confirmed by different observations such as for example the cosmic microwave background (CMB) radiation or of galaxy catalogues. However the presence of structure at smaller scales can affect local observations as it was shown in [1], and it is therefore important to understand its consequences. The effects of inhomogeneities on cosmological observables have been studied in different cases [1–24] such as dark energy, the luminosity distance [11, 12, 17] or the expansion scalar [25]. These effects are due to the fact that spatial inhomogeneities change the energy of photons, modifying the cosmological red-shift due to the Universe expansion. As a consequence some errors are produced in the estimation of parameters based on homogeneous cosmological models.

One important source of information about the Universe are galaxy catalogues since they allow to map the local density field. Since we can only measure the red-shift of astrophysical objects for which other distance measurement methods such as stellar parallax cannot be applied, it is important to take into account the effects of these inhomogeneities on the metric in order to compute self-consistently the density in red-shift space. This is particularly important when trying to determine the metric of the Universe. Different numerical [22, 26–31] and analytical [32] inversion methods have been developed in absence of the cosmological constant. More recently a numerical inversion for the luminosity distance in presence of the cosmological constant was derived in [33], but no method has been developed to reconstruct the metric from density observation in presence of a cosmological constant.

In this paper we develop for the first time a low red-shift analytical inversion method in presence of a cosmological constant to reconstruct the monopole of the metric from the monopole of the density contrast, modeling the monopole of local structure with a spherically symmetric exact solution of Einstein’s fields equations.

The paper is organized as follows. In section II we show how we model the monopole of the local structure using an exact solution of Einstein’s field equations. In section III we compute the redshift expansion of the geodesics equations [25]. In section IV we calculate the density $\rho(z)$ and the density contrast $\delta(z)$. Finally in section V we develop an analytical method to determine the metric of the Universe from the density contrast.

II. MODELING THE LOCAL UNIVERSE

In order to model the monopole component of the local structure we use the LTB solution [34–38]

$$ds^2 = -dt^2 + \frac{R'(t, r)^2}{1 + 2E(r)} dr^2 + R(t, r)^2 d\Omega^2, \quad (1)$$

where $E(r)$ is an arbitrary function of r , R is a function of the time coordinate t and the radial coordinate r , and the partial derivative of this function with respect to r is denoted as $R'(t, r) = \partial_r R(t, r)$. It follows from the Einstein's equations that

$$\left(\frac{\dot{R}}{R}\right)^2 = \frac{2E(r)}{R^2} + \frac{2M(r)}{R^3} + \frac{\Lambda}{3}, \quad (2)$$

$$\rho(t, r) = \frac{2M'}{R^2 R'}, \quad (3)$$

where $M(r)$ is an arbitrary function of the radial coordinate r , we adopt a system of units in which $c = 8\pi G = 1$, and we denote the partial derivative of R with respect to t as $\dot{R} = \partial_t R(t, r)$.

To compute any quantity in redshift space, in particular $\rho(z)$ and $\delta(z)$, we need to solve the radial null geodesics [39]

$$\frac{dr}{dz} = \frac{\sqrt{1 + 2E(r(z))}}{(1 + z)\dot{R}[t(z), r(z)]}, \quad (4)$$

$$\frac{dt}{dz} = -\frac{R'[t(z), r(z)]}{(1 + z)\dot{R}[t(z), r(z)]}. \quad (5)$$

The analytical solution of eq.(2) can be derived [40, 41] if we introduce new functions $\rho_0(r)$ and $k(r)$, and a new coordinate $\eta = \eta(t, r)$ given by

$$\frac{\partial \eta}{\partial t} \Big|_r = \frac{r}{R} = \frac{1}{a}, \quad (6)$$

$$\rho_0(r) = \frac{6M(r)}{r^3}, \quad (7)$$

$$k(r) = -\frac{2E(r)}{r^2}. \quad (8)$$

Without any loss of generality we will adopt the coordinate system in which $\rho_0(r)$ is a constant, which is known as the FLRW gauge. Then we can express eq.(2) in the form

$$\left(\frac{\partial a}{\partial \eta}\right)^2 = -k(r)a^2 + \frac{\rho_0}{3}a + \frac{\Lambda}{3}a^4, \quad (9)$$

The coordinate η is defined implicitly by eq.(6), and can be considered a generalization of the conformal time in a FLRW Universe. Therefore if we integrate this equation we can find the relation between η and t given by [20]

$$t(\eta, r) = \int_0^\eta a(x, r) dx + t_b(r), \quad (10)$$

where $t_b(r)$ is a functional constant of integration known as the bang function, because it corresponds to the fact that the scalar factor in this solution can vanish at different times at different radius. We will just consider models in which the scale factor vanishes at the same time at all radius, ie. $t_b(r) = 0$. Then we can write the solution of eq.(9) in the form

$$a(\eta, r) = \frac{\rho_0}{k(r) + 3\wp(\frac{\eta}{2}; g_2(r), g_3(r))}, \quad (11)$$

where $\wp(x; g_2, g_3)$ is the Weierstrass elliptic function and

$$g_2(r) = \frac{4}{3}k(r)^2, \quad g_3(r) = \frac{4}{27}(2k(r)^3 - \Lambda\rho_0^2). \quad (12)$$

In terms of the new coordinate η and the function $a(\eta, r)$ the radial null geodesics are given by [5]

$$\frac{d\eta}{dz} = -\frac{\partial_r t(\eta, r) + G(\eta, r)}{(1+z)\partial_\eta G(\eta, r)}, \quad (13)$$

$$\frac{dr}{dz} = \frac{a(\eta, r)}{(1+z)\partial_\eta G(\eta, r)}, \quad (14)$$

where the function $G(\eta, r)$ has an explicit analytical form, making the above geodesics equations particularly suitable for a low-red-shift expansion, and is given by

$$G(\eta, r) \equiv \frac{R'(t(\eta, r), r)}{\sqrt{1 - k(r)r^2}}, \quad (15)$$

$$R'(t(\eta, r), r) = \partial_r(a(\eta, r)r) - a^{-1}\partial_\eta(a(\eta, r)r)\partial_r t(\eta, r). \quad (16)$$

Finally, in terms of the new coordinate system the density profile is given by

$$\rho(\eta, r) = \rho(t(\eta, r), r) = \frac{\rho_0}{a(\eta, r)^2 R'(t(\eta, r), r)}, \quad (17)$$

where $R'(t(\eta, r), r)$ is given in eq.(16).

III. ANALYTICAL APPROXIMATIONS

In order to obtain a low-redshift formula for the density contrast and the density profile we expand the function $k(r)$ as

$$k(r) = k_0 + k_1 r + k_2 r^2 + \dots, \quad (18)$$

From the exact solution for $a(\eta, r)$ we can obtain an expansion for $t(\eta, r)$ according to

$$t(\eta, r) = t_0(r) + a(\eta_0, r)(\eta - \eta_0) + \frac{1}{2}\partial_\eta a(\eta_0, r)(\eta - \eta_0)^2 + \dots, \quad (19)$$

where we defined $t_0(r)$ by

$$t_0(r) \equiv t(\eta_0, r). \quad (20)$$

On the other hand the integral in eq.(10) can be computed using the properties of the Weierstrass elliptic functions \wp , ζ and σ [42], and is given by [25]

$$t(\eta, r) = \frac{2\rho_0}{3\wp' \left(\wp^{-1} \left(-\frac{k(r)}{3} \right) \right)} \left[\ln \left(\frac{\sigma \left(\frac{\eta}{2} - \wp^{-1} \left(-\frac{k(r)}{3} \right) \right)}{\sigma \left(\frac{\eta}{2} + \wp^{-1} \left(-\frac{k(r)}{3} \right) \right)} \right) + \eta \zeta \left(\wp^{-1} \left(-\frac{k(r)}{3} \right) \right) \right], \quad (21)$$

where \wp' is the derivative of the Weierstrass' elliptic function \wp . \wp^{-1} , ζ and σ are defined according to the following relations

$$\wp^{-1}(\wp(x)) = x, \quad (22)$$

$$\zeta'(x) = -\wp(x), \quad (23)$$

$$\frac{\sigma'(x)}{\sigma(x)} = \zeta(x). \quad (24)$$

Now we introduce the dimensionless quantities K_n , given by $k_n = K_n(a_0 H_0)^{n+2}$, and applying the chain rule for the derivatives of $t_0(r)$ it follows from eq.(20) and (21) that

$$t'_0(0) = \frac{\partial t_0(r)}{\partial r} \Big|_{r=0} = \left(\frac{\partial t_0}{\partial k} \frac{\partial k}{\partial r} \right) \Big|_{r=0} = a_0 \alpha K_1, \quad (25)$$

$$t''_0(0) = a_0(a_0 H_0) (\beta K_1^2 + 2\alpha K_2), \quad (26)$$

where α and β are dimensionless quantities given by

$$\alpha = \frac{(a_0 H_0)^3}{a_0} \frac{\partial t_0}{\partial k} \Big|_{k=k_0}, \quad (27)$$

$$\beta = \frac{(a_0 H_0)^5}{a_0} \frac{\partial^2 t_0}{\partial k^2} \Big|_{k=k_0}. \quad (28)$$

Now the low red-shift Taylor expansion for the geodesic equations can be found [12]. In order to do this the solution of the geodesic equations is expanded according to

$$r(z) = r_1 z + r_2 z^2 + r_3 z^3 + \dots \quad (29)$$

$$\eta(z) = \eta_0 + \eta_1 z + \eta_2 z^2 + \dots \quad (30)$$

The solution of the system of differential equations given by the geodesic equations can be mapped into the solution of a system of algebraic equations for the coefficients of the expansions

shown in eq.(29) and (30) after substituting these expansions in eq.(13) and (14) . Here we will consider the case in which $k_0 = 0$, which is enough to understand qualitatively the effects of the inhomogeneity, since this term corresponds to the homogeneous component of the curvature function $k(r)$. Indeed when there is no inhomogeneity k_0 is just the curvature of a *FLRW* solution and therefore is not related to any new physical effect not already known from the standard cosmological model.

We get for the geodesics then:

$$\eta_1 = -\frac{\alpha K_1 + 1}{a_0 H_0}, \quad (31)$$

$$\eta_2 = \frac{1}{12a_0 H_0 \Omega_M} [2K_1^2 (-4\alpha + 9\alpha^2 (\Omega_M - 1) \Omega_M - 3\beta \Omega_M) + K_1 (27\alpha \Omega_M^2 - 12\alpha \Omega_M - 4) + 3\Omega_M (3\Omega_M - 4\alpha K_2)], \quad (32)$$

$$r_1 = \frac{1}{a_0 H_0}, \quad (33)$$

$$r_2 = \frac{K_1 (-18\alpha \Omega_M^2 + 12\alpha \Omega_M + 4) - 9\Omega_M^2}{12a_0 H_0 \Omega_M}, \quad (34)$$

$$\begin{aligned} r_3 = \frac{1}{72a_0 H_0 \Omega_\Lambda \Omega_M^2} [& 2K_1^2 (4\zeta_0 + \Omega_\Lambda (-27(8\alpha^2 + \beta) \Omega_M^3 + 18(3\alpha^2 - 4\alpha + \beta) \Omega_M^2 + \\ & + 162\alpha^2 \Omega_M^4 + 36\alpha \Omega_M + 4) - 6\zeta_0 \Omega_M + 2\Omega_M) + 12K_1 \Omega_\Lambda \Omega_M^2 (27\alpha \Omega_M^2 - 24\alpha \Omega_M - 5) + \\ & + 3\Omega_\Lambda \Omega_M (K_2 (-36\alpha \Omega_M^2 + 24\alpha \Omega_M + 8) + 3(9\Omega_M - 4) \Omega_M^2)] . \end{aligned} \quad (35)$$

In the above equations we have used [9]

$$\rho_0 = 3\Omega_M a_0^3 H_0^2, \quad (36)$$

$$\Lambda = 3\Omega_\Lambda H_0^2, \quad (37)$$

$$T_0 = \eta_0 (a_0 H_0), \quad (38)$$

$$a_0 = a(\eta_0, 0), \quad (39)$$

$$H_0 = H(\eta_0, 0), \quad (40)$$

$$\zeta_0 = \zeta \left(\frac{T_0}{2}; \frac{4K_0^2}{3}, \frac{4}{27} (2K_0^3 - 27\Omega_\Lambda \Omega_M^2) \right), \quad (41)$$

where ζ is the Weierstrass Zeta Function.

The effects of the inhomogeneity start to show respectively at first order for $\eta(z)$ and second order for $r(z)$ as can be seen from the formulae we found.

IV. FORMULAE FOR THE DENSITY PROFILE AND DENSITY CONTRAST AT LOW REDSHIFT

The density profile in redshift space is given by

$$\rho(z) = \rho(\eta(z), r(z)), \quad (42)$$

and substituting the formulae for $\eta(z), r(z)$ we obtain after expanding to second order in redshift

$$\rho(z) = 3\Omega_M H_0^2 + \rho_1 z + \rho_2 z^2, \quad (43)$$

$$\rho_1 = H_0^2 (4K_1 (3\alpha\Omega_M + 1) + 9\Omega_M), \quad (44)$$

$$\begin{aligned} \rho_2 = & -\frac{H_0^2}{12\Omega_\Lambda\Omega_M} [K_1^2 (\Omega_\Lambda (-18 (25\alpha^2 - 4\alpha + 5\beta) \Omega_M^2 + 81\alpha^2 \Omega_M^3 - 300\alpha\Omega_M - 40) + \\ & + 20 (\Omega_M - \zeta_0)) + 18K_1\Omega_\Lambda\Omega_M (3\alpha\Omega_M^2 + (2 - 24\alpha)\Omega_M - 8) + \\ & - 12\Omega_\Lambda\Omega_M (5K_2 (3\alpha\Omega_M + 1) + 9\Omega_M)] . \end{aligned} \quad (45)$$

In order to derive an analytical approximation for the density contrast we must first define what is the background density of the Universe, which is given by the volume average of ρ

$$\bar{\rho}(z) = \frac{\int_V \rho(t(z), r) dV}{\int_V dV} = \frac{\int_0^\infty \rho(t(z), r) \frac{R(t(z), r)^2 R'(t(z), r)}{\sqrt{1-k(r)r^2}} dr}{\int_0^\infty \frac{R(t(z), r)^2 R'(t(z), r)}{\sqrt{1-k(r)r^2}} dr}. \quad (46)$$

The density contrast is then defined as

$$\delta(z) = \frac{\rho(z)}{\bar{\rho}(z)} - 1. \quad (47)$$

If the size of the local inhomogeneity is sufficiently smaller than the volume over which the integral in eq.(46) is performed then $\bar{\rho}$ will get most of its contribution from the asymptotically homogeneous region and the average density will be well approximated by the asymptotic density

$$\bar{\rho}(z) = 3(H_0^b)^2 \Omega_M^b (1+z)^3, \quad (48)$$

where the upper-script ^b stands for background. This is clearly true for compensated structure of any size, but it also applies to uncompensated structures whose size is sufficiently smaller

than the asymptotic homogeneous region. In this paper we will consider compensated structure when comparing to numerical results, but the formulae we derive can also be applied to uncompensated structures when the conditions explained above are satisfied.

Expanding the density contrast we find

$$\delta(z) = \delta_0 + \delta_1 z + \delta_2 z^2, \quad (49)$$

$$\delta_0 = \left(\frac{H_0}{H_0^b} \right)^2 \left(\frac{\Omega_M}{\Omega_M^b} - 1 \right), \quad (50)$$

$$\delta_1 = \left(\frac{H_0}{H_0^b} \right)^2 \frac{4K_1 (3\alpha\Omega_M + 1)}{3\Omega_M^b}, \quad (51)$$

$$\delta_2 = - \left(\frac{H_0}{H_0^b} \right)^2 \frac{1}{36\Omega_M^b \Omega_\Lambda \Omega_M} [K_1^2 (\Omega_\Lambda (-18 (25\alpha^2 - 4\alpha + 5\beta) \Omega_M^2 + 81\alpha^2 \Omega_M^3 - 300\alpha\Omega_M +$$

$$-40) + 20 (\Omega_M - \zeta_0)) + 18K_1 \Omega_\Lambda \Omega_M^2 (3\alpha\Omega_M + 2) - 60K_2 \Omega_\Lambda \Omega_M (3\alpha\Omega_M + 1)]. \quad (52)$$

As can be seen the first order coefficients of the expansion of $\rho(z)$ and $\delta(z)$ depend on K_1 , while the second order depend on both K_1 and K_2 .

The procedure to reduce the analytical formulae to this form is rather complicated since it involves to express wherever possible all the intermediate expressions in terms of physically meaningful quantities and we give more details about it in appendix A. The formulae for the case in which k_0 is different from zero are rather cumbersome and we give them in appendix B.

A. Comparison with numerical and perturbative calculations

In order to test the formulae we have derived in the previous section we consider inhomogeneities defined by a spatial curvature function $k(r)$ of this type

$$k(r) = \pm \frac{r}{5} [1 - \tanh(2r)], \quad (53)$$

which is plotted in fig.(1). We solve numerically eq.(2) and the null geodesic equations in eq.(4) and (5). This type of function $k(r)$ is satisfying the assumption we made in the previous section that $k(0) = k_0 = 0$ and it corresponds to compensated structures making it easy to define background quantities according to eq.(46). We can then define the background parameters H_0^b and Ω_M^b as

$$H_0^b = \overline{H}(0), \quad \text{and} \quad \Omega_M^b = \frac{\overline{\rho}(0)}{3(H_0^b)^2}, \quad (54)$$

where the quantity $\overline{H}(z)$ is defined through the same volume average given in eq.(46) applied to $H(t, r)$ [25] instead of $\rho(t, r)$. For the models we consider we have $H_0^b = H_0$ and $\Omega_M^b = \Omega_M$.

For compensated inhomogeneities the asymptotic behavior of the function $k(r)$ allows to define background quantities also as

$$\bar{\rho}(z) = \lim_{r \rightarrow \infty} \rho(t(z), r). \quad (55)$$

$$\bar{H}(z) = \lim_{r \rightarrow \infty} H(t(z), r). \quad (56)$$

For the models in eq.(53) it also follows that the curvature of the background solution is $k^b = \lim_{r \rightarrow \infty} k(r) = 0$, which corresponds to a flat homogeneous Universe.

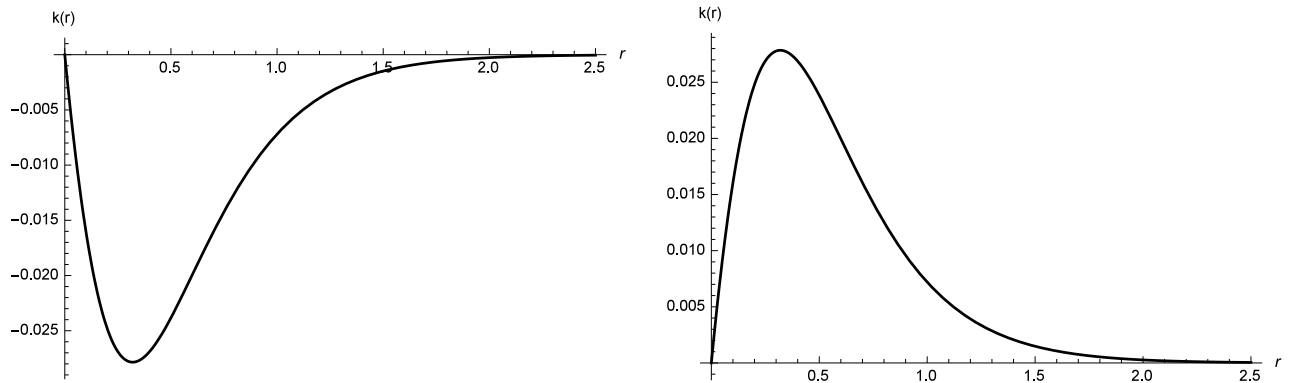


FIG. 1: The function $k(r)$ defined in eq.(53) is plotted in units of H_0^2 as a function of the radial coordinate in units of H_0^{-1} .

In order to compare our results to linear perturbation theory we compute the perturbation theory prediction for $\delta(z)$ according to [43]

$$\delta(z) \approx -3\delta H(z)(\Omega_M^b)^{-0.55}. \quad (57)$$

As can be seen in fig.(3) and fig.(2) at low red-shift the analytical formulae for $\rho(z)$ and $\delta(z)$ derived in eq.(43) and (49) are in good agreement with the numerical calculations and are more accurate than the perturbation theory prediction in eq.(57).

V. RECONSTRUCTION OF THE METRIC FROM THE DENSITY CONTRAST

In the previous section we have obtained the red-shift expansion of the density contrast in terms of the coefficients dimensionless coefficient K_i , and we will now use this to solve the inversion problem, i.e. to obtain K_i from the density contrast. Note that in the the coefficients K_i complete determine the metric, so that we will be able to reconstruct the metric from the density contrast.

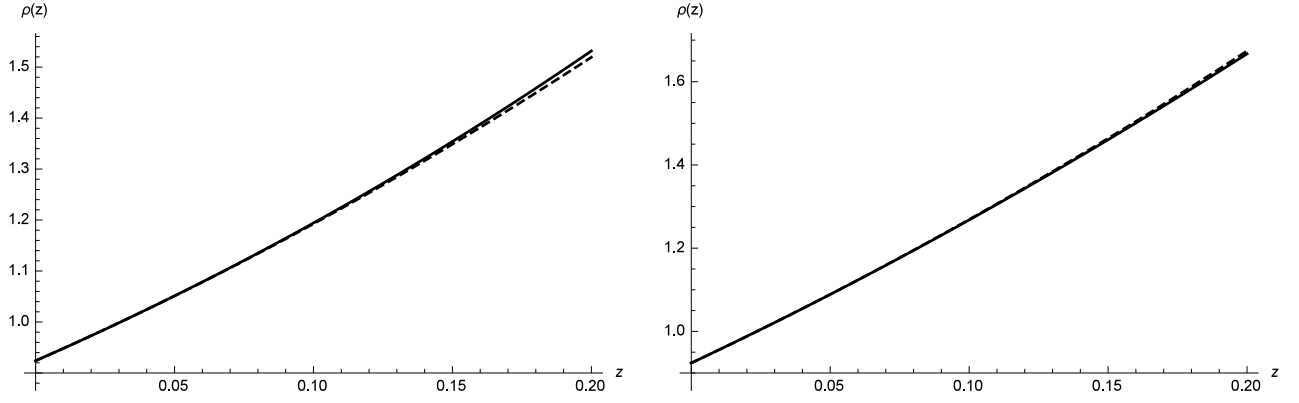


FIG. 2: The density profile in units of H_0^2 is plotted as a function of redshift. The left and right are plots are for the inhomogeneities corresponding to Fig. 1. The solid lines are for the numerical calculation and the dashed lines for the analytical approximation.

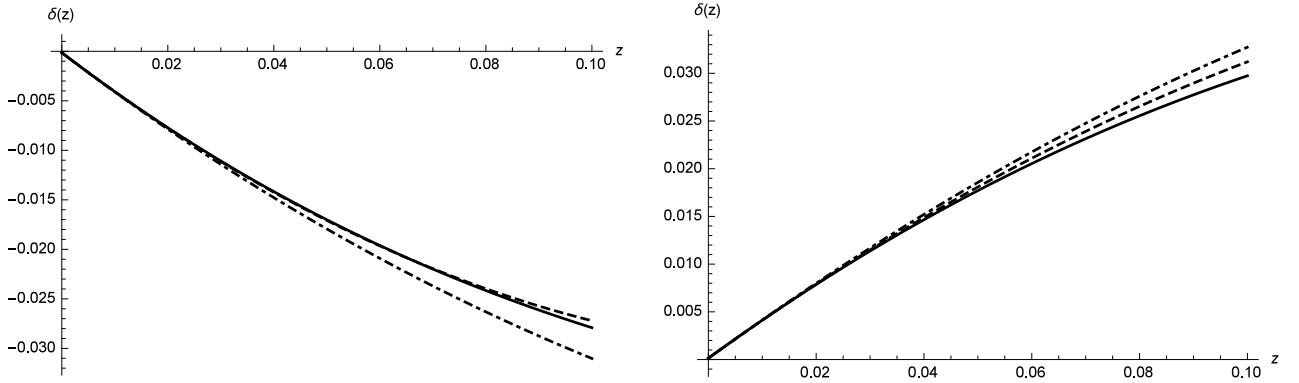


FIG. 3: The density contrast is plotted as a function of redshift. The left and right plots are for the inhomogeneities corresponding to Fig. 1. The solid lines correspond to the numerical solution, the dashed lines to the analytical formula we derived and the dot-dashed lines to the perturbation theory result.

From eq.(50) we get

$$\Omega_M^b = \frac{\Omega_M}{(1 + \delta_0)} \left(\frac{H_0}{H_0^b} \right)^2, \quad (58)$$

and after replacing it in eq.(51) and (52) we can solve the system of equations for the

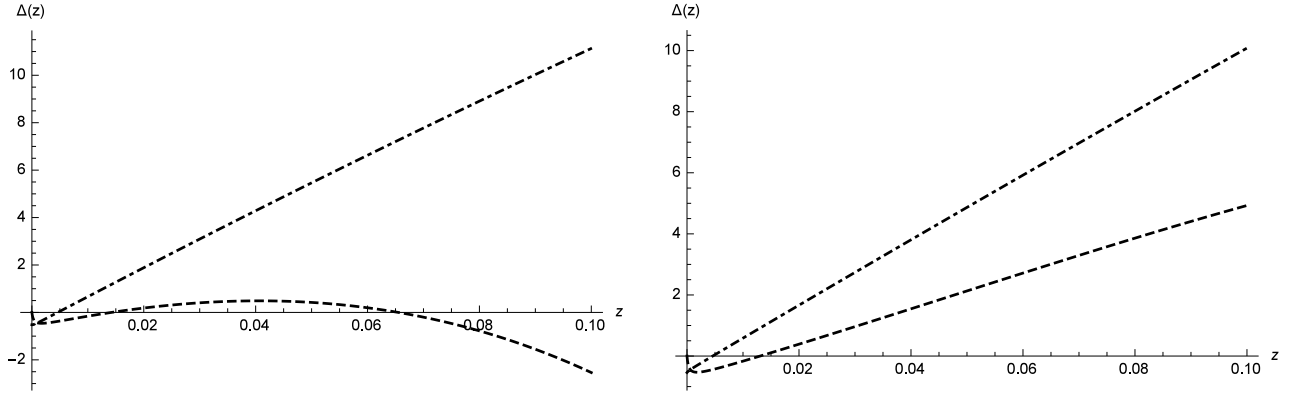


FIG. 4: The relative percentual difference between different analytical approximations and the numerical calculation $\Delta(z) = 100 \left(\frac{\delta^A(z)}{\delta^N(z)} - 1 \right)$ is plotted as a function of redshift. The left and right plots correspond to inhomogeneities in Fig. 1. The dashed lines are for the analytical formula and the dot-dashed lines for the perturbation theory approximation.

coefficient of the $k(r)$ expansion K_1 and K_2

$$k(r) \approx K_1 (a_0 H_0)^3 r + K_2 (a_0 H_0)^4 r^2, \quad (59)$$

$$K_1 = \frac{3\delta_1 \Omega_M}{4(\delta_0 + 1)(3\alpha\Omega_M + 1)}, \quad (60)$$

$$K_2 = \frac{3\Omega_M}{320(\delta_0 + 1)^2 \Omega_\Lambda (3\alpha\Omega_M + 1)^3} [\Omega_\Lambda (8(\delta_0 + 1)\delta_2 - 5\delta_1^2) - 18\Omega_M^2 (\alpha^2 (25\delta_1^2 + \\ -32(\delta_0 + 1)\delta_2) - 4\alpha\delta_1 (3\delta_0 + \delta_1 + 3) + 5\beta\delta_1^2) + 27\alpha^2\delta_1 (8\delta_0 + 3\delta_1 + 8)\Omega_M^3 + \\ + 12(-25\alpha\delta_1^2 + 32\alpha(\delta_0 + 1)\delta_2 + 4(\delta_0 + 1)\delta_1)\Omega_M) + 20\delta_1^2(\Omega_M - \zeta_0)]. \quad (61)$$

The linear coefficient K_1 depends on both δ_0 and δ_1 , while the second order coefficient K_2 depends also on δ_2 . This is naturally expected since a homogeneous Universe corresponds to $K_1 = K_2 = \delta_1 = \delta_2 = 0$. As a consistency check it can be easily verified that in fact $K_1 = K_2 = 0$ in the homogeneous limit, i.e. when $\delta_1 = \delta_2 = 0$.

A. Testing the accuracy of the inversion method

In order to test the inversion method we compute numerically the density using the models defined in eq.(53) and then calculate the corresponding low red-shift expansion of $\delta(z)$. The coefficients of the reconstructed $k(r)$ are then obtained from eq.(59). The result of the inversion is then compared to the original $k(r)$ defined in eq.(53). As shown in fig.(5) at low red-shift the reconstructed $k(r)$ is in good agreement with the numerical results.

As shown in the previous section the perturbative calculation for $\delta(z)$ is less accurate than the analytical formula we computed in eq.(51-52). We can infer that also the perturbative solution of the inversion problem, which would consist in solving the perturbed Einstein's equations to get the metric from the density contrast, will be less accurate than the analytical method we have developed.

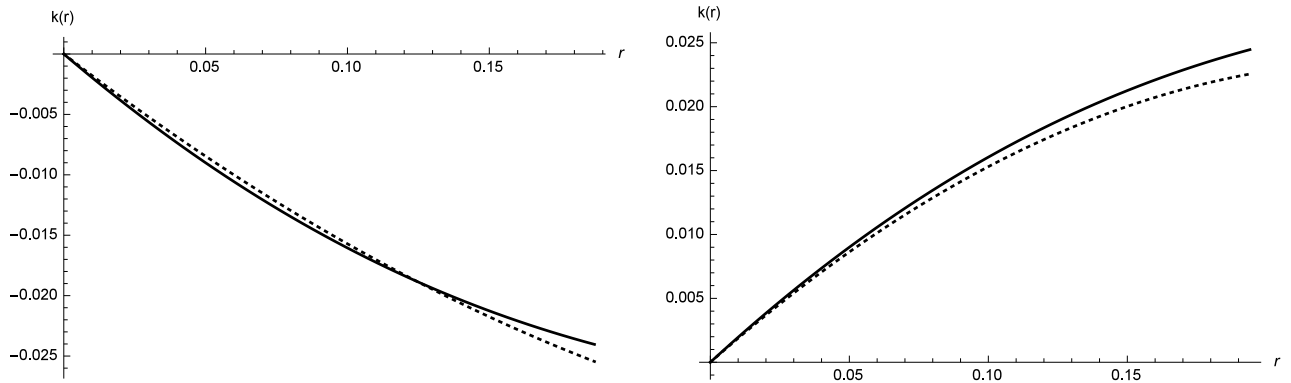


FIG. 5: The reconstructed metric function $k(r)$ is plotted in units of H_0^2 as a function of the radial coordinate in units of H_0^{-1} for the inhomogeneities corresponding to Fig 1. The black solid line corresponds to the original $k(r)$ function and the black dotted line to the reconstructed one.

VI. CONCLUSIONS

We have derived the low-redshift expansion for the monopole of the density profile and the density contrast. At low red-shift the formulae are in good agreement with numerical solutions and are more accurate than the linear perturbation theory approximation. Using these formulae we have then developed a new analytical inversion method to reconstruct the monopole of the metric from the monopole of the density contrast. The inversion method could be applied to low red-shift observational data to determine the metric with a level of precision higher than the one achievable using perturbation theory.

In the future the formulae we obtained for the metric could be used in the expansion of other cosmological observables to get coordinate independent formulas for these quantities in terms of the density contrast, without the need to expand the metric. It will also be interesting to develop a numerical inversion method able to reconstruct the metric beyond the regime of validity of the low red-shift expansion or to adopt other more accurate expansion techniques

such as the Padé approximation.

For a full reconstruction of the metric beyond the monopole contribution other solutions of the Einstein's equations could be used for the analytical approach, in order to accommodate more complex geometries. For a general numerical inversion able to reconstruct any type of metric more sophisticated methods in numerical relativity will be required.

Appendix A: Derivation of the analytical formula

In order to obtain the formulae for the red-shift expansion of $\rho(z)$ and $\delta(z)$ we have applied several manipulations and substitutions. The method is based on re-expressing everything in terms of physical quantities, starting from the definitions of a_0 and H_0 , which are related to \wp and \wp' by the equations

$$a_0 \equiv (\eta_0, 0) = \frac{\rho_0}{k_0 + 3\wp_0}, \quad (1)$$

$$H_0 \equiv H(\eta_0, 0) = -\frac{3\wp'_0}{2\rho_0}, \quad (2)$$

$$(3)$$

where

$$\wp_0 = \wp(\eta_0; g_2(0), g_3(0)), \quad (4)$$

$$\wp'_0 = \frac{\partial \wp(\eta; g_2(0), g_3(0))}{\partial \eta} \Big|_{\eta=\eta_0}. \quad (5)$$

By inverting the previous equations we obtain the following relations

$$\wp_0 = \wp(\eta_0; g_2(0), g_3(0)) = \frac{\rho_0 - a_0 k_0}{3a_0}, \quad (6)$$

$$\wp'_0 = \frac{\partial \wp(\eta; g_2(0), g_3(0))}{\partial \eta} \Big|_{\eta=\eta_0} = -\frac{2H_0 \rho_0}{3}. \quad (7)$$

We can then substitute the above expressions everywhere \wp and \wp' appear, making the final formula only depending on physical quantities such as H_0 .

In order to simplify the results we have also used the Einstein's equation at the center $(\eta_0, 0)$

$$1 = -K_0 + \Omega_M + \Omega_\Lambda. \quad (8)$$

Appendix B: General formulae

Here we give the low red-shift formulae for the density and for the solution to the inversion problem for the general case in which k_0 is different from zero.

For the density profile we have

$$\rho(z) = 3H_0^2\Omega_M + \rho_1 z + \rho_2 z^2, \quad (1)$$

$$\rho_1 = \frac{3H_0^2\Omega_M}{27\Omega_\Lambda\Omega_M^2 - 4K_0^3} [-4K_0^3(4\alpha K_1 + 3) + 9\Omega_\Lambda\Omega_M(4K_1(3\alpha\Omega_M + 1) + 9\Omega_M) + 24K_1K_0(\zeta_0 - \Omega_M) + 4K_1K_0^2(T_0 + 2)], \quad (2)$$

$$\begin{aligned} \rho_2 = & \frac{3H_0^2\Omega_M}{4(4K_0^3 - 27\Omega_M^2\Omega_\Lambda)^2} [-16(K_1(T_0 + 4) - 12)K_0^6 + 2(T_0(3T_0 + 16)K_1^2 + \\ & + 12((T_0 + 12)\Omega_M - 4(2T_0 + \zeta_0 + 4))K_1 - 40K_2(T_0 + 2))K_0^5 + ((8(24\zeta_0 + 35) + \\ & + T_0(8(5T_0 + 9\zeta_0 + 25) - 9(T_0 + 16)\Omega_M))K_1^2 + 144(\Omega_M(\zeta_0 - 2\Omega_M - 2\Omega_\Lambda + 9) + \\ & - 8\zeta_0)K_1 + 480K_2(\Omega_M - \zeta_0))K_0^4 + 12((18\zeta_0^2 + (40(T_0 + 3) - 9(T_0 + 8)\Omega_M)\zeta_0 + \\ & + \Omega_M(T_0(12\Omega_M + 12\Omega_\Lambda - 43) - 126))K_1^2 + 9\Omega_M((T_0 + 8)\Omega_M - 16)\Omega_\Lambda K_1 + \\ & - 12\Omega_M(5K_2 + 18\Omega_M)\Omega_\Lambda)K_0^3 - 18(2(-40\zeta_0^2 + 6\Omega_M^2(-4\zeta_0 + T_0\Omega_\Lambda - 6) + \\ & + \Omega_M(\zeta_0(9\zeta_0 + 86) - (20T_0 + 24\zeta_0 + 75)\Omega_\Lambda + 5))K_1^2 + 9\Omega_M^2((T_0 + 12)\Omega_M + \\ & - 4(2T_0 + \zeta_0 + 4))\Omega_\Lambda K_1 - 30K_2(T_0 + 2)\Omega_M^2\Omega_\Lambda)K_0^2 + 108\Omega_M\Omega_\Lambda((40\zeta_0 + (5T_0 + \\ & - 12\zeta_0 - 28)\Omega_M)K_1^2 + 9\Omega_M(8\zeta_0 + \Omega_M(-\zeta_0 + 2\Omega_M + 2\Omega_\Lambda - 9))K_1 + 30K_2(\zeta_0 + \\ & - \Omega_M)\Omega_M)K_0 + ((6K_0 - 9\Omega_M + 50)\alpha^2 + 10\beta)K_1^2 + 20\alpha K_2)(4K_0^3 - 27\Omega_M^2\Omega_\Lambda)^2 + \\ & + 324\Omega_M^2\Omega_\Lambda(5(\zeta_0 - \Omega_M + 2\Omega_\Lambda)K_1^2 - 9(\Omega_M - 4)\Omega_M\Omega_\Lambda K_1 + 3\Omega_M(5K_2 + \\ & + 9\Omega_M)\Omega_\Lambda) + 2\alpha K_1(4K_0^3 - 27\Omega_M^2\Omega_\Lambda)(8K_0^4 - 2(K_1(3T_0 + 8) + 6(\Omega_M - 8))K_0^3 + \\ & + K_1(-50(T_0 + 2) - 36\zeta_0 + 9(T_0 + 8)\Omega_M)K_0^2 + 6K_1\zeta_0(9\Omega_M - 50)K_0 + \\ & - 6\Omega_M(9\Omega_M\Omega_\Lambda + K_1(12\Omega_M + 12\Omega_\Lambda - 53))K_0 + 9\Omega_M(9(\Omega_M - 8)\Omega_M + \\ & + 2K_1(6\Omega_M - 25))\Omega_\Lambda)]. \end{aligned} \quad (3)$$

The low red-shift expansion for the density contrast is

$$\delta(z) = \delta_0 + \delta_1 z + \delta_2 z^2, \quad (4)$$

$$\delta_0 = \left(\frac{H_0}{H_0^b} \right)^2 \left(\frac{\Omega_M}{\Omega_M^b} - 1 \right), \quad (5)$$

$$\delta_1 = - \left(\frac{H_0}{H_0^b} \right)^2 \frac{4K_1\Omega_M(-4\alpha K_0^3 + 6K_0(\zeta_0 - \Omega_M) + K_0^2(T_0 + 2) + 9\Omega_\Lambda\Omega_M(3\alpha\Omega_M + 1))}{\Omega_M^b(4K_0^3 - 27\Omega_\Lambda\Omega_M^2)}, \quad (6)$$

$$\begin{aligned} \delta_2 = & \left(\frac{H_0}{H_0^b} \right)^2 \frac{\Omega_M}{4\Omega_M^b(4K_0^3 - 27\Omega_\Lambda\Omega_M^2)^2} [(4K_0^3 - 27\Omega_\Lambda\Omega_M^2)^2 (20\alpha K_2 + K_1^2(10\beta + \alpha^2(6K_0 + \\ & -9\Omega_M + 50))) + 324\Omega_\Lambda\Omega_M^2(5K_1^2(\zeta_0 + 2\Omega_\Lambda - \Omega_M) - 9K_1\Omega_\Lambda\Omega_M^2 + 15K_2\Omega_\Lambda\Omega_M) + \\ & + 2\alpha K_1(4K_0^3 - 27\Omega_\Lambda\Omega_M^2)(6\zeta_0 K_1 K_0(9\Omega_M - 50) - 6K_0\Omega_M(K_1(12\Omega_\Lambda + 12\Omega_M + \\ & -53) + 9\Omega_\Lambda\Omega_M) + 9\Omega_\Lambda\Omega_M(2K_1(6\Omega_M - 25) + 9\Omega_M^2) + K_1K_0^2(-36\zeta_0 + 9(T_0 + \\ & + 8)\Omega_M - 50(T_0 + 2)) - 2K_0^3(K_1(3T_0 + 8) + 6\Omega_M) + 8K_0^4) + K_0^4(144K_1\Omega_M(\zeta_0 + \\ & -2\Omega_\Lambda - 2\Omega_M + 1) + 480K_2(\Omega_M - \zeta_0) + K_1^2(8(24\zeta_0 + 35) + T_0(8(9\zeta_0 + 5T_0 + 25) + \\ & -9(T_0 + 16)\Omega_M))) + 12K_0^3(-60K_2\Omega_\Lambda\Omega_M + K_1^2(18\zeta_0^2 + \zeta_0(40(T_0 + 3) - 9(T_0 + \\ & + 8)\Omega_M) + \Omega_M(T_0(12\Omega_\Lambda + 12\Omega_M - 43) - 126)) + 9K_1(T_0 + 8)\Omega_\Lambda\Omega_M^2) + \\ & - 18K_0^2(2K_1^2(-40\zeta_0^2 + 6\Omega_M^2(-4\zeta_0 + T_0\Omega_\Lambda - 6) + \Omega_M(\zeta_0(9\zeta_0 + 86) - \Omega_\Lambda(24\zeta_0 + \\ & + 20T_0 + 75) + 5)) + 9K_1\Omega_\Lambda\Omega_M^2((T_0 + 12)\Omega_M - 4\zeta_0) - 30K_2(T_0 + 2)\Omega_\Lambda\Omega_M^2) + \\ & + 108K_0\Omega_\Lambda\Omega_M(9K_1\Omega_M^2(-\zeta_0 + 2\Omega_\Lambda + 2\Omega_M - 1) + 30K_2\Omega_M(\zeta_0 - \Omega_M) + K_1^2(40\zeta_0 + \\ & + \Omega_M(-12\zeta_0 + 5T_0 - 28))) + K_0^5(2K_1(-48\zeta_0 + K_1T_0(3T_0 + 16) + 12(T_0 + \\ & + 12)\Omega_M) - 80K_2(T_0 + 2)) - 16K_1K_0^6(T_0 + 4)]. \end{aligned} \quad (7)$$

The solution of the inversion problem is

$$k(r) = (a_0 H_0)^2 K_0 + (a_0 H_0)^3 K_1 r + (a_0 H_0)^4 K_2 r^2, \quad (8)$$

$$K_1 = \frac{\delta_1 (4K_0^3 - 27\Omega_\Lambda \Omega_M^2)}{4(\delta_0 + 1)\mathcal{A}}, \quad (9)$$

$$K_2 = -\frac{(4K_0^3 - 27\Omega_M^2 \Omega_\Lambda)}{320(\delta_0 + 1)^2 \mathcal{A}^3} [32\alpha^2 \delta_1 (8\delta_0 + 3\delta_1 + 8) K_0^7 - 16((-50\delta_1^2 + 3(8\delta_0 + 3\delta_1 + 8)\Omega_M \delta_1 + 64(\delta_0 + 1)\delta_2)\alpha^2 + \delta_1(8(3\delta_0 + \delta_1 + 3) + T_0(8\delta_0 + 3\delta_1 + 8))\alpha + 10\beta\delta_1^2) K_0^6 + 2((3T_0^2 + 4(\alpha(9\Omega_M - 50) + 4)T_0 + 16\alpha(-9\zeta_0 + 18\Omega_M - 25))\delta_1^2 + 8(\delta_0 + 1)(T_0^2 + 6(2\alpha\Omega_M + 1)T_0 - 48\alpha\zeta_0 + 108\alpha\Omega_M + 8)\delta_1 + 256\alpha(T_0 + 2)(\delta_0 + 1)\delta_2) K_0^5 - (144\alpha\delta_1(4(3\delta_0 + \delta_1 + 3) + 3\alpha(8\delta_0 + 3\delta_1 + 8)\Omega_\Lambda)\Omega_M^2 + 3((3T_0^2 + 48T_0 + 16\alpha(-9\zeta_0 + 12\Omega_\Lambda - 53))\delta_1^2 + 8(\delta_0 + 1)(T_0^2 + 18T_0 + 8(\alpha(-6\zeta_0 + 9\Omega_\Lambda - 3) + 5))\delta_1 + 1024\alpha(\delta_0 + 1)\delta_2)\Omega_M - 8(-8(\delta_0 + 1)\delta_2(T_0 + 2)^2 + 5(T_0^2 + 5T_0 + 7)\delta_1^2 + 3((-100\alpha + 3T_0 + 8)\delta_1^2 + 8(T_0 + 3)(\delta_0 + 1)\delta_1 + 128\alpha(\delta_0 + 1)\delta_2)\zeta_0)) K_0^4 + 12(54\alpha^2\delta_1(8\delta_0 + 3\delta_1 + 8)\Omega_\Lambda\Omega_M^3 + 3(384(\delta_0 + 1)\delta_2\Omega_\Lambda\alpha^2 + 4(\delta_0 + 1)\delta_1(6\alpha\Omega_\Lambda T_0 + 3T_0 + 36\alpha\Omega_\Lambda + 16) + \delta_1^2(T_0(9\alpha\Omega_\Lambda + 4) - 12(25\alpha^2 + 4\alpha + 5\beta)\Omega_\Lambda))\Omega_M^2 + ((T_0(-9\zeta_0 + 12\Omega_\Lambda - 43) - 6(12\zeta_0 + 50\alpha\Omega_\Lambda + 21))\delta_1^2 + 12(\delta_0 + 1)(-2\zeta_0 T_0 - T_0 - 18\zeta_0 + (3T_0 + 8)\Omega_\Lambda - 2)\delta_1 + 64(\delta_0 + 1)\delta_2(T_0 + 6\alpha\Omega_\Lambda + 2))\Omega_M + 2\zeta_0(3\delta_1(8\delta_0 + 3\delta_1 + 8)\zeta_0 - 4(8(T_0 + 2)(\delta_0 + 1)\delta_2 + 5(T_0 + 3)\delta_1^2))) K_0^3 - 18(3\delta_1(32(\delta_0 + 1) + 3\alpha(24(3\delta_0 + \delta_1 + 3) + T_0(8\delta_0 + 3\delta_1 + 8))\Omega_\Lambda)\Omega_M^3 - 2(3(8\zeta_0 + ((25\alpha - 2)T_0 + 2\alpha(9\zeta_0 + 25))\Omega_\Lambda + 12)\delta_1^2 - 6(\delta_0 + 1)(3(T_0 - 8\alpha\zeta_0 + 8)\Omega_\Lambda - 4(3\zeta_0 + 1))\delta_1 - 32(\delta_0 + 1)\delta_2(3\alpha(T_0 + 2)\Omega_\Lambda + 2))\Omega_M^2 + 2(-5(4T_0\Omega_\Lambda + 15\Omega_\Lambda - 1)\delta_1^2 + 3(8\delta_0 + 3\delta_1 + 8)\zeta_0^2\delta_1 + 32(T_0 + 2)(\delta_0 + 1)\delta_2\Omega_\Lambda - 2\zeta_0((12\Omega_\Lambda - 43)\delta_1^2 + 12(\delta_0 + 1)(3\Omega_\Lambda - 1)\delta_1 + 64(\delta_0 + 1)\delta_2))\Omega_M + 16(8(\delta_0 + 1)\delta_2 - 5\delta_1^2)\zeta_0^2) K_0^2 + 54\Omega_M\Omega_\Lambda(9\alpha\delta_1(8(3\delta_0 + \delta_1 + 3) + 3\alpha(8\delta_0 + 3\delta_1 + 8)\Omega_\Lambda)\Omega_M^3 + 6(\alpha(-9\zeta_0 + 12\Omega_\Lambda - 53)\delta_1^2 + 4(\delta_0 + 1)(\alpha(-6\zeta_0 + 9\Omega_\Lambda - 3) + 4)\delta_1 + 64\alpha(\delta_0 + 1)\delta_2)\Omega_M^2 + 2((5T_0 + 150\alpha\zeta_0 - 12\zeta_0 - 28)\delta_1^2 + 12(\delta_0 + 1)(-3\zeta_0 + 2\Omega_\Lambda - 1)\delta_1 - 64(\delta_0 + 1)\delta_2(3\alpha\zeta_0 - 1))\Omega_M + 16(5\delta_1^2 - 8(\delta_0 + 1)\delta_2)\zeta_0) K_0 - 81\Omega_M^2\Omega_\Lambda(20(\Omega_M - \zeta_0)\delta_1^2 + (27\alpha^2\delta_1(8\delta_0 + 3\delta_1 + 8)\Omega_M^3 + 18((25\delta_1^2 - 32(\delta_0 + 1)\delta_2)\alpha^2 - 4\delta_1(3\delta_0 + \delta_1 + 3)\alpha + 5\beta\delta_1^2)\Omega_M^2 + 12(-25\alpha\delta_1^2 + 4(\delta_0 + 1)\delta_1 + 32\alpha(\delta_0 + 1)\delta_2)\Omega_M + 8(8(\delta_0 + 1)\delta_2 - 5\delta_1^2))\Omega_\Lambda)] , \quad (10)$$

where we have defined

$$\mathcal{A} = 4\alpha K_0^3 - (T_0 + 2) K_0^2 + 6 (\Omega_M - \zeta_0) K_0 - 9\Omega_M (3\alpha\Omega_M + 1) \Omega_\Lambda . \quad (11)$$

Acknowledgments

- [1] A. Enea Romano and S. Andrés Vallejo, EPL (Europhysics Letters) **109**, 39002 (2015), arXiv:1403.2034.
- [2] A. E. Romano, S. Sanes, and M. Sasaki, (2013), arXiv:1311.1476.
- [3] C. Clarkson and M. Regis, JCAP **1102**, 013 (2011), arXiv:1007.3443.
- [4] A. E. Romano, Phys.Rev. **D75**, 043509 (2007), arXiv:astro-ph/0612002.
- [5] A. E. Romano and M. Sasaki, Gen.Rel.Grav. **44**, 353 (2012), arXiv:0905.3342.
- [6] I. Ben-Dayan, R. Durrer, G. Marozzi, and D. J. Schwarz, Phys.Rev.Lett. **112**, 221301 (2014), arXiv:1401.7973.
- [7] M. Redlich, K. Bolejko, S. Meyer, G. F. Lewis, and M. Bartelmann, Astron.Astrophys. **570**, A63 (2014), arXiv:1408.1872.
- [8] A. E. Romano, JCAP **1001**, 004 (2010), arXiv:0911.2927.
- [9] A. E. Romano, Int.J.Mod.Phys. **D21**, 1250085 (2012), arXiv:1112.1777.
- [10] V. Marra and A. Notari, Class.Quant.Grav. **28**, 164004 (2011), arXiv:1102.1015.
- [11] A. E. Romano and P. Chen, JCAP **1110**, 016 (2011), arXiv:1104.0730.
- [12] A. E. Romano, M. Sasaki, and A. A. Starobinsky, Eur.Phys.J. **C72**, 2242 (2012), arXiv:1006.4735.
- [13] A. Krasiski, Phys.Rev. **D90**, 023524 (2014), arXiv:1405.6066.
- [14] A. E. Romano, Gen.Rel.Grav. **45**, 1515 (2013), arXiv:1206.6164.
- [15] A. E. Romano, Int.J.Mod.Phys. **D21**, 1250085 (2012), arXiv:1112.1777.
- [16] A. Balcerzak and M. P. Dabrowski, (2013), arXiv:1310.7231.
- [17] A. E. Romano and P. Chen, Eur.Phys.J. **C74**, 2780 (2014), arXiv:1207.5572.
- [18] A. E. Romano and M. Sasaki, General Relativity and Gravitation **44**, 353 (2012), arXiv:0905.3342.
- [19] G. Fanizza, M. Gasperini, G. Marozzi, and G. Veneziano, JCAP **1311**, 019 (2013), arXiv:1308.4935.
- [20] Romano, Antonio Enea and Chen, Pisin, Eur. Phys. J. C **74**, 2780 (2014).

- [21] A. Krasiski, Phys.Rev. **D90**, 103525 (2014), arXiv:1409.5377.
- [22] D. J. H. Chung and A. E. Romano, Phys. Rev. **D74**, 103507 (2006), arXiv:astro-ph/0608403.
- [23] A. E. Romano, H.-W. Chiang, and P. Chen, Class.Quant.Grav. **31**, 115008 (2014).
- [24] V. Marra, L. Amendola, I. Sawicki, and W. Valkenburg, Phys.Rev.Lett. **110**, 241305 (2013), arXiv:1303.3121.
- [25] A. E. Romano and S. A. Vallejo, European Physical Journal C **76**, 216 (2016), arXiv:1502.07672.
- [26] A. E. Romano, H.-W. Chiang, and P. Chen, Class. Quant. Grav. **31**, 115008 (2014), arXiv:1312.4458.
- [27] M.-N. Celerier, K. Bolejko, and A. Krasinski, Astron. Astrophys. **518**, A21 (2010), arXiv:0906.0905.
- [28] C.-M. Yoo, T. Kai, and K.-i. Nakao, Prog. Theor. Phys. **120**, 937 (2008), arXiv:0807.0932.
- [29] K. Bolejko, C. Hellaby, and A. H. A. Alfedeel, JCAP **1109**, 011 (2011), arXiv:1102.3370.
- [30] M. L. McClure and C. Hellaby, Phys. Rev. **D78**, 044005 (2008), arXiv:0709.0875.
- [31] N. Mustapha, C. Hellaby, and G. F. R. Ellis, Mon. Not. Roy. Astron. Soc. **292**, 817 (1997), arXiv:gr-qc/9808079.
- [32] A. E. Romano, Phys. Rev. **D82**, 123528 (2010), arXiv:0912.4108.
- [33] M. Tokutake and C.-M. Yoo, JCAP **1610**, 009 (2016), arXiv:1603.07837.
- [34] G. Lemaître, Annales de la Société Scientifique de Bruxelles **53** (1933).
- [35] G. Lemaitre, Gen.Rel.Grav. **29**, 641 (1997).
- [36] G. Lemaitre, Mon. Not. Roy. Astron. Soc. **91**, 490 (1931).
- [37] R. C. Tolman, Proc.Nat.Acad.Sci. **20**, 169 (1934).
- [38] H. Bondi, Mon. Not. Roy. Astron. Soc. **107**, 410 (1947).
- [39] M.-N. Celerier, Astron.Astrophys. **353**, 63 (2000), arXiv:astro-ph/9907206.
- [40] A. Zecca, Adv.Stud.Theor.Phys. **7**, 1101 (2013).
- [41] D. Edwards, Monthly Notices of the Royal Astronomical Society **159**, 51 (1972).
- [42] M. Abramowitz and I. A. Stegun, *Handbook of Mathematical Functions with Formulas, Graphs, and Mathematical Tables*, tenth dover printing ed. (Dover, New York, 1972).
- [43] E. L. Turner, R. Cen, and J. P. Ostriker, Astrophys.J. **103**, 1427 (1992).